

Journal of Biomedical Optics

SPIDigitalLibrary.org/jbo

Analyzing reflectance spectra of human skin in legal medicine

Liudmila Belenki
Vera Sterzik
Katharina Schulz
Michael Bohnert



SPIE

Analyzing reflectance spectra of human skin in legal medicine

Liudmila Belenki,^a Vera Sterzik,^b Katharina Schulz,^c and Michael Bohnert^b

^aUniversity of Freiburg, Materials Research Center Freiburg, Stefan-Meier-Straße 21, 79104 Freiburg, Germany

^bUniversity of Würzburg, Institute of Legal Medicine, Versbacher Street 3, 97078 Würzburg, Germany

^cUniversity of Freiburg, Institute of Legal Medicine, Albertstraße 9, 79104 Freiburg, Germany

Abstract. Our current research in the framework of an interdisciplinary project focuses on modelling the dynamics of the hemoglobin reoxygenation process in post-mortem human skin by reflectance spectrometry. The observations of reoxygenation of hemoglobin in livores after postmortem exposure to a cold environment relate the reoxygenation to the commonly known phenomenon that the color impression of livores changes from livid to pink under low ambient temperatures. We analyze the spectra with respect to a physical model describing the optical properties of human skin, discuss the dynamics of the reoxygenation, and propose a phenomenological model for reoxygenation. For additional characterization of the reflectance spectra, the curvature of the local minimum and maximum in the investigated spectral range is considered. There is a strong correlation between the curvature of spectra at a wavelength of 560 nm and the concentration of O₂-Hb. The analysis is carried out via C programs, as well as MySQL database queries in Java EE, JDBC, Matlab, and Python. © 2013 Society of Photo-Optical Instrumentation Engineers (SPIE). [DOI: [10.1117/1.JBO.18.1.017004](https://doi.org/10.1117/1.JBO.18.1.017004)]

Keywords: reflectance spectrometry; optical properties; physical model of human skin; reoxygenation of hemoglobin in livores; data analysis.

Paper 12518TN received Aug. 14, 2012; revised manuscript received Nov. 6, 2012; accepted for publication Nov. 26, 2012; published online Jan. 7, 2013.

1 Introduction

For modern medicine and biomedical sciences, it is important to have fast, noninvasive techniques for differential diagnosis or fundamental research at hand. One successfully applied method is reflectance spectrometry. It is the most important method for analyzing skin *in vivo*¹⁻⁴ and for the age determination of a traumatic injuries.^{5,6} In dermatology, this approach is used for the differential diagnosis of malignant melanoma,⁷ while in legal and forensic medicine, it helps to estimate the cooling process and to confirm that the discoloration of livor mortis due to cooling is caused by reoxygenation of hemoglobin.^{1,8,9} The color qualities of pink livores seen after exposure to a cold environment and in carbon monoxide (CO) poisoning are very similar. Nevertheless, by means of spectrometric measurements and statistical data analysis based on a physical skin model, it is possible to distinguish between two possibilities.

Postmortem lividity is the earliest apparent sign of death. Therefore, the first step in clarifying the change of color is to investigate the different states of cooled and uncooled livores by reflectance spectrometry.^{10,11} Here, the discolored skin is irradiated with a white light source of a known intensity spectrum that is comparable to bright daylight. The intensity of the reflected light is determined for each wavelength in the visible range. The livid color of livor mortis results from a nearly complete consumption of hemoglobin-bound oxygen (O₂-Hb) during agony. It is a well-known phenomenon that the appearance of livor mortis changes to a bright red or pink color under low ambient temperatures.¹²⁻¹⁶ This corresponds to a qualitative change of the reflectance curve that occurs in the wavelength

range between 500 and 600 nm.^{1,5,6,8,9} In order to explain this observation, most textbooks draw on the theory that oxygen diffuses from ambient air into the skin vessels and binds to hemoglobin molecules.^{13,17-19} This theory has been substantiated by experimental results of Bohnert et al.⁸ and Watchman et al.,⁹ which have been obtained by measuring the reflectance of livor mortis and analyzing the resulting spectra with respect to an optical model of human skin.^{1,9,20} Here we report the application of this approach to investigations on the dynamics of reoxygenation. More precisely, we propose a phenomenological model of the reoxygenation process.

2 Materials and Methods

2.1 Study Population

By means of reflectance spectrometry, postmortem lividity was investigated over a period of four years in 82 Caucasians brought to the Institute of Legal Medicine of the Freiburg University shortly after death. Immediately after arrival, the corpses were taken to a cold storage room of 4°C to 6°C. The study included 52 males ages 25 to 93 (mean = 54.5, median = 49.5, std = 16.9) and 30 females ages 23 to 95 (mean = 68.2, median = 72, std = 20.2).

2.2 Reflectance Spectrometry

If one looks at an unknown material, one important property being recognized is the color. This intuitive material characterization can be specified by reflectance spectrometry. Spectral reflectance reveals a lot of subtle information about the microstructure of the material, like the concentration of

Address all correspondence to: Liudmila Belenki, University of Freiburg, Materials Research Center Freiburg, Stefan-Meier-Straße 21, 79104 Freiburg, Germany. Tel: +49 (151) 28478362; E-mail: liudmila.belenki@gmail.com

0091-3286/2013/\$25.00 © 2013 SPIE

light-absorbing substances and the size distribution of light-scattering structures.

Measurements were performed with the diode array spectrophotometer MCS 400 (Carl-Zeiss-Jena GmbH, Jena, Germany) and a halogen bulb as light source (standard illuminant D65). The spectral resolution is 0.8 nm within the wavelength range of 188 to 1018 nm. The measuring head allowed recording of the directed surface reflection of a 5-mm-wide measurement spot. Compressed barium sulphate was used as white standard according to ISO 7724-2. Furthermore, the measurements were controlled and evaluated via the control software ASPECT+ running on a personal computer. Reflectance was saved in the range of 350 to 750 nm. The reflectance spectrometry and skin temperature measurements were performed on livores located in the lateral region of the thorax and on pallor (uncolored skin) located on the breast forewall. Further parameters recorded were time of death, cause of death, start of refrigeration, body mass index, age, and gender. Measurements were performed at intervals ranging from 6 to 12 h. The reflectance spectra have been managed via a scientific information repository as described by Belenkaia et al.²¹ Altogether, 357 measurements were carried out, with 241 being used for correlation analysis. These 241 reflectance curves obtained from 82 bodies were analyzed with respect to the physical skin model described below.

2.3 Estimation of O_2 -Hb Concentrations

In all cases, the color impression of postmortem lividity changed from livid to bright red in the course of cooling the corpses. Furthermore, for every case, the respective reflectance spectra of the livores evolved the described local maximum between 500 and 600 nm. With this observation in mind, the question arises of whether it is possible to determine the concentration of Hb and O_2 -Hb by means of the reflectance spectrum. In order to obtain this not directly accessible information, one has to relate the mesoscopic material properties to the optical properties of the skin and furthermore model the dependency of the reflectance on the optical skin properties. The latter can be parameterized by the absorption coefficient μ_a , the scattering coefficient μ_s' , and the anisotropy factor g . While the absorption coefficient is determined by the concentration and the extinction spectrum of Hb, O_2 -Hb, and CO-Hb,^{22–24} the scattering coefficient and the anisotropy factor can be modelled in terms of the Mie theory^{25,26} if one assumes the shape of the light-scattering obstacles (e.g., mitochondria) to be spherical. Now, the dependency of the reflectance on the optical material parameters can be determined by a Monte-Carlo model simulating the light transport in a turbid medium.¹ The Monte-Carlo-based calibration model was estimated for a semi-infinite half-space with a refractive index of $n_1 = 1.36$. The reflectance $R(\mu_s', \mu_a)$ was calculated for a detector radius of $r = 0.5$ cm. The human skin is a very complex organ with a three-layered structure consisting of the stratum corneum, the stratum germinativum, and the dermis. The thin stratum corneum causes regular reflectance at tissue-air transition. This regular reflectance is due to the refractive index mismatch between the stratum corneum ($n_{sc} = 1.55$) and air ($n_{air} = 1.0$). In the visible light range, skin reflects between 4% and 7% of the incident beam, nearly independent of wavelength and skin type.²² The stratum germinativum und dermis are composed of many organelles and substructures that influence the transport of light. However, the main scattering processes are elastic scattering processes by mitochondria and collagen fibers that can be described by a scatterer²⁷ with

diameter d within the interval (0.1, 0.8) μm and a refractive index of $n_2 = 1.4$. The effective particle size distribution $h(d)$ of the scatter (mitochondria) was calculated within the interval (0.1, 0.8) with a discretisation of $\Delta d = 0.1$ μm . In the visible range of light, the absorption processes are mainly due to hemoglobin. Due to the cold, O_2 binds more easily to hemoglobin, and its release to the tissue is impeded.²²

The extinction spectra of Hb, O_2 -Hb, and CO-Hb were taken into account for the modelling of the absorption coefficient. In a first approximation, the human skin can be modeled as a turbid, absorbing, semi-infinite medium composed of homogeneously distributed scatterers and absorbers. Given this correlation, the microscopic parameters can be estimated from a measured reflectance spectrum by inversion using least-square or regularization methods in a range of 500 to 600 nm,^{1,20} because this range contains the typical minima and maxima for deoxygenated and oxygenated hemoglobin. The standard deviations were calculated under the assumption of Gaussian error propagation. The reflectance spectra that were measured in the range of 350 to 750 nm, as well as their respective meta data, like case number, age, gender, etc., were stored in a scientific information repository,²¹ from which the primary data were retrieved for data analysis and in which the estimated skin parameters were saved. The analysis is carried out via C programs,⁷ as well as via MySQL database queries in Java EE, JDBC, Matlab, and Python. Statistical analysis was performed with SPSS Statistics 19.0.0 (IBM Corporation, Somers, New York), with $P < 0.05$ considered as statistically significant.

3 Results

3.1 One Example of the Discoloration via Cooling Down

An example of livor mortis taken from a 89-year-old Caucasian female is described here. One and a half hours after death, the corpse was brought into a cold environment of approximately 5°C. The first picture of postmortem lividity, shown in Fig. 1(a), was taken after 24 h of cooling. At that time, the hypostatic areas were greyish-blue, and the skin had cooled down to 10.9°C. A very different color impression of this discoloration will be observed if the corpse continues cooling down. At a skin temperature of 8°C, as shown in Fig. 1(b), the livores exhibit a pink color. While the livid color of uncooled livor mortis resembles the mixture of red and blue, the origin of the combination color pink cannot be determined by the naked eye, due to the many different ways of creating a pink color impression.²⁸ A series of five reflectance spectra of postmortem lividity measured at different skin temperatures in the course of cooling down the corpse is shown in Fig. 1(c). For temperatures higher than 10°C, shown by curves T_1 and T_2 in Fig. 1(c), the broad reflectance plateau in the wavelength region corresponding to orange/red colors is obvious. The same holds for the prominent reflectance peak in the blue color regime. These regions of large reflectance are separated by a reflectance minimum masking the green/yellow part of the spectrum. Obviously, the reflectance maxima located at wavelengths corresponding to blue and red colors result in the livid color impression of uncooled livores shown in Fig. 1(a). In the course of the skin's cooling down, the reflectance spectra change such that the local maximum of the blue reflectance region shifts to larger wavelengths resembling a blue/green color, and the reflectance plateau of the large wavelength regime evolves a prominent peak at its left border

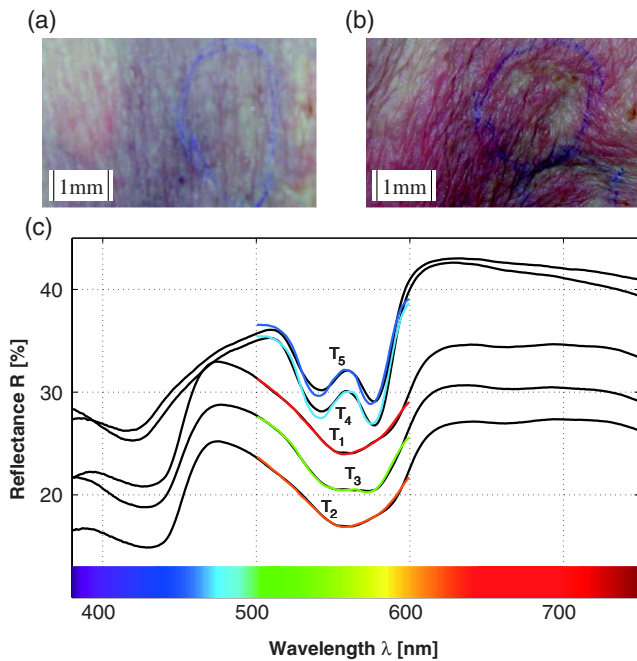


Fig. 1 Appearance of livores for decreasing skin temperature. Images of livores observed at a skin temperature of (a) 10.9°C and (b) 8.0°C. Blue lines mark areas being characterised by reflectance spectroscopy. (c) Reflectance spectra recorded at skin temperatures $T_1 = 10.9^\circ\text{C}$, $T_2 = 10.3^\circ\text{C}$, $T_3 = 8.6^\circ\text{C}$, $T_4 = 8.0^\circ\text{C}$, and $T_5 = 7.5^\circ\text{C}$. Superimposed colored curves indicate the reflectance estimated on the basis of the physical model. Although the base line of the reflectance spectra differs from measurement to measurement, the evolving local maximum at wavelengths resembling a yellow-green color impression is apparent for decreasing skin temperature.

corresponding to an orange color impression, shown by curves T_3 , T_4 , and T_5 in Fig. 1(c). A qualitative change of the reflectance spectra can be observed for intermediate colors (500 to 600 nm), where a new local maximum of reflectance rises at 560 nm. This local maximum being flanked by two local minima at 541 and 576 nm is a typical feature of oxygenated hemoglobin,^{9,22} suggesting a high concentration of $\text{O}_2\text{-Hb}$ within the cooled livor mortis. Superimposed colored curves indicate the reflectance estimated on the basis of the physical model.

Now we consider a series of five reflectance spectra of pallor (uncolored skin) measured at the same skin temperatures as for lividity in the course of cooling down the corpse (Fig. 2). For temperatures higher than 10°C, shown by curves T_1 , T_2 and T_3 in Fig. 2, flat reflectance minima and maxima in the wavelength region of 380 to 750 nm are observed. For low temperatures $T_4 = 8.0^\circ\text{C}$ and $T_5 = 7.5^\circ\text{C}$, a local minimum of reflectance rises at 576 nm, and a very weak local minimum rises at 541 nm, suggesting a low concentration of oxygenated hemoglobin $\text{O}_2\text{-Hb}$ within the cooled pallor.

A series of absorption coefficients μ_a and scattering coefficients μ'_s in dependency on the wavelength were estimated⁷ via the program TMinv at the same skin temperatures as the five reflectance spectra from Fig. 1(c) and are shown in Figs. 3 and 4. A qualitative change of the absorption coefficient is observed in the range of 500 to 600 nm. Double peaks arise around 541 and 576 nm (Fig. 3). This result is the same as those found by Garcia-Urbe et al. and Watchman et al.^{2,9} The latter corresponds to the maximum and minimum of the corresponding reflectance curve at the same wavelengths. In contrast

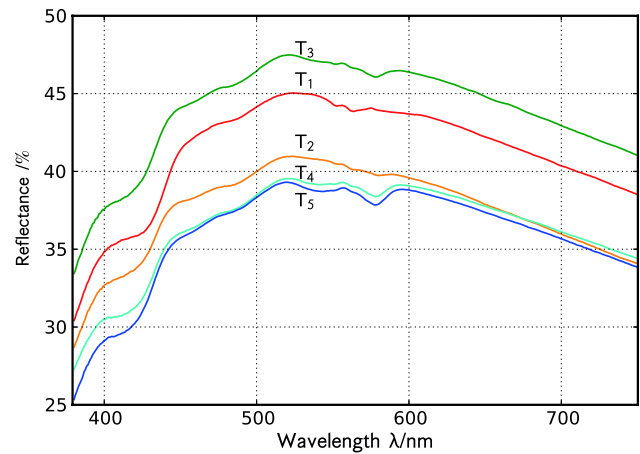


Fig. 2 Reflectance spectra of pallor (uncolored skin) recorded at skin temperatures $T_1 = 10.9^\circ\text{C}$, $T_2 = 10.3^\circ\text{C}$, $T_3 = 8.6^\circ\text{C}$, $T_4 = 8.0^\circ\text{C}$, and $T_5 = 7.5^\circ\text{C}$. For temperatures higher than 8.0°C (curves T_1 , T_2 , and T_3), the platy reflectance extrema for intermediate colors (500 to 600 nm) are observed. For temperatures lower than 8.0°C (curves T_4 and T_5), a local minimum appears at 576 nm. Additionally, a very weak local minimum at 541 nm can be observed.

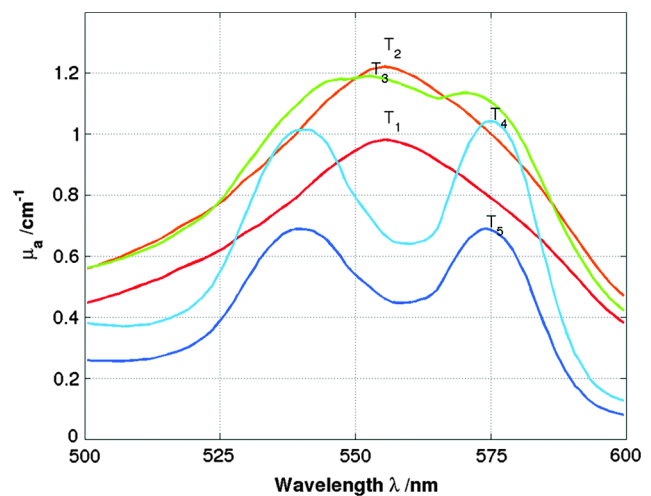


Fig. 3 The optical parameter absorption coefficient μ_a was determined by the concentration and the extinction spectrum of Hb, $\text{O}_2\text{-Hb}$, and CO-Hb at skin temperatures $T_1 = 10.9^\circ\text{C}$, $T_2 = 10.3^\circ\text{C}$, $T_3 = 8.6^\circ\text{C}$, $T_4 = 8.0^\circ\text{C}$, and $T_5 = 7.5^\circ\text{C}$ in dependency on the wavelength.

to the behavior of the absorption coefficients, the scattering coefficients are in linear dependency on the wavelength (Fig. 4). A similar behavior of μ'_s was observed by Garcia-Urbe et al.²

3.2 Dynamics of Reoxygenation for an Exemplary Case

Applying the Monte-Carlo model to the exemplary case discussed in Fig. 1, the time series of $\text{O}_2\text{-Hb}$ concentrations presented in Fig. 5 is achieved. The dynamics reveal two phases of livore appearance. The first phase starts with the cooling down of the corpse and is characterized by a negligible $\text{O}_2\text{-Hb}$ concentration. The first phase of our exemplary case occurs from 24 to 34 h after the beginning of cooling, at which time the skin temperature decreases from 10.9°C to 10.3°C (black squares in Fig. 5). For this interval, the $\text{O}_2\text{-Hb}$ concentration is less than

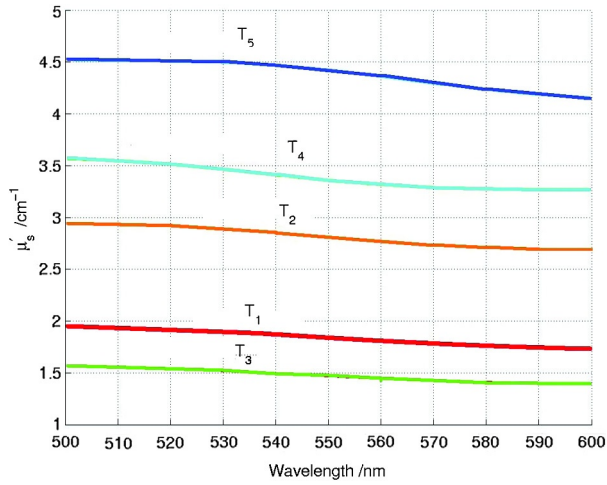


Fig. 4 The reduced scattering coefficient μ'_s was calculated in dependency on the wavelength at the same skin temperatures as the parameter μ_a (see Fig. 3).

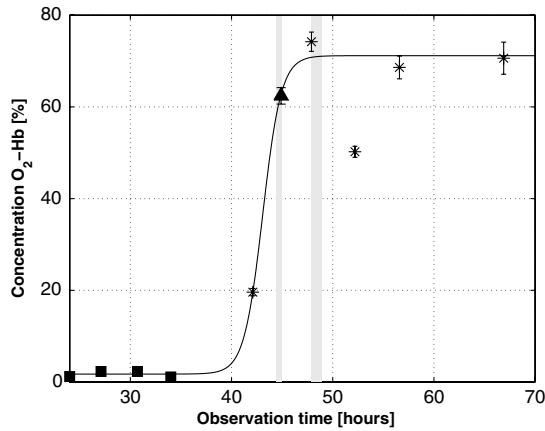


Fig. 5 Time series of O_2 -Hb concentration for the discussed case documenting the changing color of livores due to cooling. The concentrations are estimated from reflectance spectra of livores (Fig. 1) measured in the course of cooling down the corpse. The respective skin temperature is indicated by symbols. Asterix: 7°C to 9°C, black boxes: 10°C to 11°C, black triangle: 11.9°C. Shaded regions mark intervals of warming at room temperature. Estimation errors are calculated from error propagation. In case of low O_2 -Hb-concentrations, the error bars lie within the symbol bounds. The symbol on the far left and the second symbol on the right correspond to Fig. 1(a) and 1(b), respectively.

2.5%. The second phase starts with the measurement taken 42 h after the beginning of cooling, at which time the concentration of O_2 -Hb has increased to approximately 20%, while the skin temperature has decreased to 8.6°C. In the further course of time, the concentration of O_2 -Hb within the livores reaches a level of approximately 70%. From this final state of saturation, the image of bright red livores shown in Fig 1(b) was taken.

We found that transitions from low to high O_2 -Hb concentrations in the course of the cooling down of the corpse are generic and can be described by

$$c_{O_2Hb}(t) = \frac{\Delta c}{2} \left\{ 1 + \tanh \left[\frac{2c_s}{\Delta c} (t - t_0) \right] \right\} + c_{min}, \quad (1)$$

where t denotes the cooling duration in hours, c_{min} is the minimal O_2 -Hb concentration percentage, Δc is the increase of the O_2 -Hb concentration percentage, t_0 is the inflection point of the model function at which the concentration has reached half-height, and $c_s = \frac{d}{dt} c_{O_2Hb}(t)|_{t=t_0}$ is the slope of the model function at the inflection point. As can be seen in Fig. 5, the body was exposed to fluctuating ambient temperatures. Table 1 contains data for t_0 , c_{min} , Δc , c_s , χ^2 , and age for five other examples in which there were no disturbances in ambient temperature. For the shown case, the parameters of Eq. (1) can be estimated with neglect of these temperature fluctuations to $t_0 = (43.080 \pm 0.002)h$, $c_{min} = (1.74 \pm 0.05)\%$, $\Delta c = (69.42 \pm 0.14)\%$, and $c_s = (18.90 \pm 0.012)\%/h$. The cost function of this estimation sums up to $\chi^2 = 6.2$, which indicates that the estimated model (black curve in Fig. 5) fits the data well.

3.3 Temperature and Cooling Duration Dependency of Reoxygenation of Livores Within a Field Study

We analyzed 241 reflectance curves with respect to the described physical skin model, and the resulting estimated O_2 -Hb concentrations were plotted against the respective skin temperatures (Fig. 6) and the cooling duration (Fig. 7). In these diagrams, blue and magenta colored symbols indicate reflectance curves with one (blue) or three local extrema (magenta) between 500 and 600 nm being associated with bluish and red livores, respectively.

3.4 Curvature Dependency of Reoxygenation of Livores Within a Field Study

For additional characterization of the reflectance spectra, the curvature of the local minima and maxima in the investigated

Table 1 Estimated models.

| Case | $\Delta c/\%$ | t_0/h | $c_s/\%/h$ | $c_{min}/\%$ | χ^2 | Age |
|-------|-----------------|------------------|-------------------|------------------|----------|-----|
| 06254 | 69.4 ± 0.14 | 43.08 ± 0.00 | 18.9 ± 0.01 | 1.74 ± 0.05 | 6.2 | 89 |
| 05480 | 73.8 ± 0.06 | 34.1 ± 0.01 | 4.5 ± 0.00 | 0.01 ± 0.02 | 6.8 | 23 |
| 05534 | 76.1 ± 0.19 | 74.7 ± 0.01 | 6.6 ± 0.00 | 2.4 ± 0.08 | 1.9 | 85 |
| 05536 | 77.8 ± 0.12 | 40.6 ± 0.00 | 12.1 ± 0.02 | 0.008 ± 0.12 | 8.9 | 91 |
| 06058 | 74.5 ± 0.10 | 139.1 ± 0.06 | 1.9 ± 0.00005 | 3.8 ± 0.03 | 5.5 | 41 |

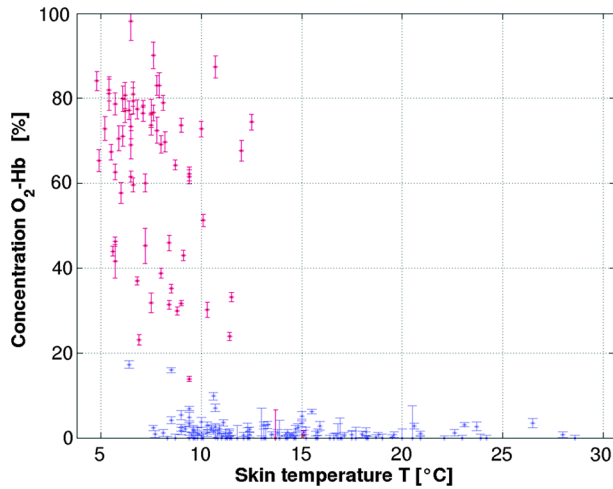


Fig. 6 Field study investigating the correlation between the temperature of livores and the concentration of O₂-Hb. The scatter plot shows 241 O₂-Hb concentrations estimated from reflectance curves obtained from 82 bodies. Livid and pink symbols refer to reflectance curves with one and three local extrema, respectively, in the wavelength interval between 500 and 600 nm.

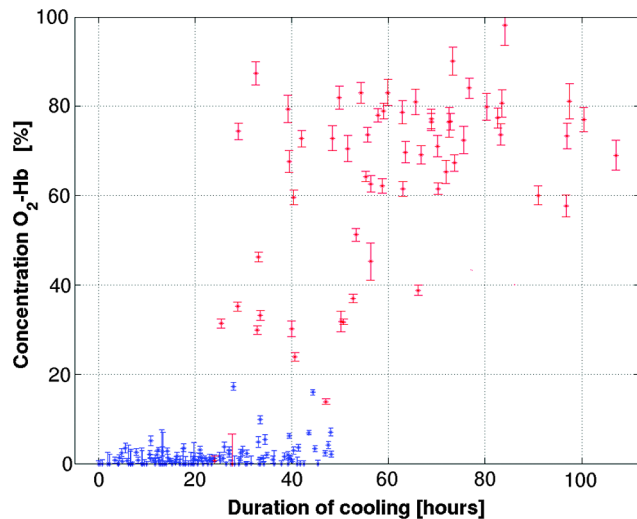


Fig. 7 Field study investigating the correlation between the duration of cooling of livores and the concentration of O₂-Hb. The scatter plot shows 241 O₂-Hb concentrations estimated from reflectance curves obtained from 82 bodies. Livid and pink symbols refer to reflectance curves with one and three local extrema, respectively, in the wavelength interval between 500 and 600 nm.

spectral range was considered. The related qualitative change of the reflectance curve can be characterized by computing the curvature at the position of the central local extremum at a wavelength of 560 nm, such that a vanishing curvature indicates the transition from one (bluish livores) to three local extrema (red livores). We consider the evolution of the curvature in dependency of the O₂-Hb concentration and carry out an analysis via MatLab (function *boxplot*). The O₂-Hb concentration is arranged into three groups: (0,20)/% (the first group), (20,60)/% (the second group), and (60,100)/% (the third group). Figure 8 shows a box plot of the curvature in relation to the O₂-Hb concentration for 241 reflectance spectra. The mean values for the three groups are 4.07 ± 1.97 , -5.67 ± 2.58 ,

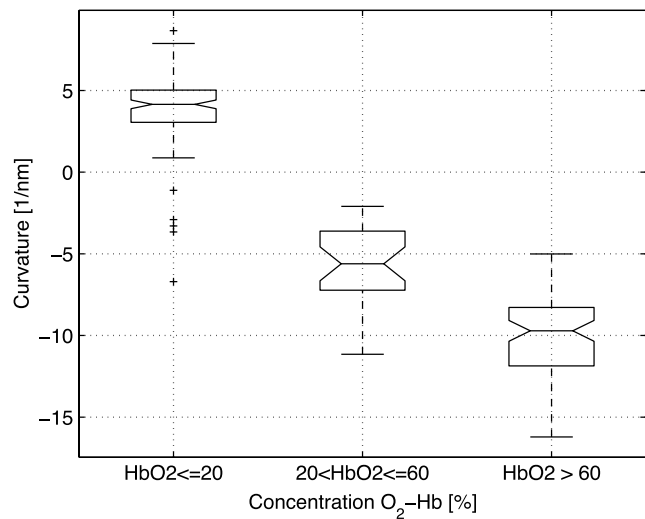


Fig. 8 Field study investigating the correlation between the curvature of reflectance spectra and O₂-Hb concentration. Box plots of the curvature in relation to the O₂-Hb concentration for 241 reflectance spectra are shown. The low O₂-Hb concentration corresponds to the positive values of the curvature with six outliers (points beyond the whiskers, which are displayed using +). Comparing the groups among each other with a Post-Hoc-Tamhane-test shows a significant difference ($p < 0.0001$): The first group of O₂-Hb concentration $\{N = 133, \text{median} = 3.8 \text{ nm}^{-1}, \text{IQR} = \{3.1; 5.0\} \text{ nm}^{-1}, \text{mean} = 4.1 \text{ nm}^{-1}, \text{std} = 1.96 \text{ nm}^{-1}\}$ and the second group of O₂-Hb concentration $\{N = 30, \text{median} = -5.6 \text{ nm}^{-1}, \text{IQR} = \{-7.4; -3.5\} \text{ nm}^{-1}, \text{mean} = -5.7 \text{ nm}^{-1}, \text{std} = 2.6 \text{ nm}^{-1}\}$ have a difference of the means = 9.7, std = 0.46. The first group and the third group of O₂-Hb concentration $\{N = 78, \text{median} = -9.7 \text{ nm}^{-1}, \text{IQR} = \{-11.9; -8.2\} \text{ nm}^{-1}, \text{mean} = -10.1 \text{ nm}^{-1}, \text{std} = 2.6 \text{ nm}^{-1}\}$ have a difference of the means = 14.2, std = 0.32. The second group and the third group have a difference of the means = 4.4, std = 0.49. Here, N is the number of reflectance curves in the corresponding group, IQR is the interquartile range, and std denotes the standard deviation.

and $-10.11 \pm 2.63 \text{ nm}^{-1}$, respectively. The curvatures in the three O₂-Hb concentration groups differed significantly ($P < 0.0001$) in the Oneway ANOVA Welch-Test. Furthermore, performing group-to-group comparisons via a Post-Hoc-Tamhane-Test showed significant between-group differences ($P < 0.0001$). Hence, there is a strong correlation between the curvature of spectra at 560 nm and the O₂-Hb concentration.

4 Conclusion

The presented investigations are based on the fact that the discoloration of livores from livid to pink due to exposure to a cold environment is related to a characteristic change of the reflectance spectrum in the wavelength interval from 500 to 600 nm. More precisely, the reflectance curve of livid livores exhibits a local minimum at 555 nm at room temperature, which evolves in the course of cooling to a local maximum at 560 nm being characteristic for the pink type of livores. These observations relate closely to the report of Bohnert et al.,⁸ who had approximated a critical temperature $T_c = (10.3 \pm 2.7)^\circ\text{C}$, which is the temperature at which the qualitative change of the reflectance curve happens.

The observed spread for the relation between skin temperature and O₂-Hb concentration is closely related to the fact that the system under investigation is not in equilibrium, but continuously transforms from its high-temperature state to its low-temperature state. This transformation is determined by the

dynamics of thermal and molecular diffusion. While thermal diffusion is driven by the temperature gradient between the warm core of the corpse and the cool environment, the molecular diffusion is driven by the gradient between oxygen-rich atmosphere and oxygen-poor livores. The overall dynamic of this relaxation process is describable by a phenomenological model that takes into account the fact that the initial and final states of the system transform into each other in a relatively short timeframe of several hours. While the structure of the model is generic, the parameters have to be adapted for each time series, because the complexity of human skin causes a certain variety of individual properties, e.g., thickness of dermal layers, which certainly affect thermal conductivity and oxygen permeability of skin. Therefore, ongoing research seeks to further improve the physical skin model and investigate the reoxygenation process with better temporal resolution. We conclude that the presented results emphasize the importance of the applied methodology combining reflectance measurements with an optical model of human skin.

Acknowledgments

This study has been supported by Deutsche Forschungsgemeinschaft (German Research Council), File No. Bo 1923/2-1. Furthermore, the authors would like to thank A. Liehr for discussion of this work and J. Honerkamp and S. Pollak for discussions at the earlier stage of this paper. We also would like to thank the anonymous reviewers for very useful remarks and fruitful advice.

References

1. M. Bohnert et al., "A Monte Carlo-based model for steady-state diffuse reflectance spectrometry in human skin: estimation of carbon monoxide concentration in livor mortis," *Int. J. Legal Med.* **119**(6), 355–362 (2005).
2. A. Garcia-Urbe et al., "In-vivo characterization of optical properties of pigmented skin lesions including melanoma using oblique incidence diffuse reflectance spectrometry," *Biomed. Opt.* **16**(2), 020501 (2011).
3. N. R. T. H. Nguyen and J. W. Tunnell, "Lookup table-based inverse model for determining optical properties of turbid media," *Biomed. Opt.* **13**(5), 050501 (2008).
4. J. A. Delgado Atencio et al., "Influence of probe pressure on human skin diffuse reflectance spectroscopy measurements," *Opt. Mem. Neural Netw.* **18**(1), 6–14 (2009).
5. L. L. Randeberg et al., "A novel approach to age determination of traumatic injuries by reflectance spectroscopy," *Lasers Surg. Med.* **38**(4), 277–289 (2006).
6. V. K. Hughes and N. E. I. Langlois, "Use of reflectance spectrophotometry and colorimetry in a general linear model for the determination of the age of bruises," *For. Sci. Med. Pathol.* **6**(4), 275–281 (2010).
7. R. Walther, "Reflexionsspektroskopie zur Charakterisierung optisch trüber Medien: Modellierung, Simulation und statistische," Datenanalyse Universität Freiburg, <http://www.freidok.uni-freiburg.de/volltexte/1309> (2004).
8. M. Bohnert et al., "Re-oxygenation of hemoglobin in livores after post-mortem exposure to a cold environment," *Int. J. Legal Med.* **122**(2), 91–96 (2008).
9. H. Watchman et al., "Re-oxygenation of post-mortem lividity by passive diffusion through the skin at low temperature," *Forensic Sci. Med. Pathol.* **7**(4), 333–335 (2011).
10. G. Kortüm, *Reflexionsspektroskopie: Grundlagen, Methodik, Anwendungen*, Springer, Berlin (1969).
11. B. Hapke, *Theory of Reflectance and Emission Spectroscopy*, p. 472, Cambridge University Press, Cambridge (2005).
12. F. J. Holzer, "Über Eigentümlichkeiten beim Rotwerden der Totenflecken," *Z. Medizinalbeamt.* **2**, 65–72 (1934).
13. H. Kessler, "Zur Differentialdiagnose der Einwirkung von Kälte oder Kohlenoxyd auf die Färbung der Hypostase," MD Thesis, Heidelberg University Press (1951).
14. W. U. Spitz, *Medicolegal Investigation of Death*, 3rd ed., Thomas, Springfield (1993).
15. V. J. M. DiMaio and D. J. DiMaio, *Forensic Pathology*, 2nd ed., CRC, Boca Raton (2001).
16. P. J. Saukko and B. Knight, *Knight's Forensic Pathology*, 3rd ed., Arnold, London (2004).
17. B. Mueller, *Gerichtliche Medizin*, 2nd ed., Springer, Heidelberg (1975).
18. B. Forster, *Praxis der Rechtsmedizin*, Thieme, Stuttgart, New York (1987).
19. B. Brinkmann and B. Madea, Eds., *Handbuch Gerichtliche Medizin*, Springer, Berlin (2003).
20. R. Walther et al., "Monte Carlo based model for steady-state diffuse reflectance spectroscopy," *Proc. SPIE* **5261**, 88–99 (2004).
21. L. Belenkaia, M. Bohnert, and A. W. Liehr, *Electronic Laboratory Notebook Assisting Reflectance Spectrometry in Legal Medicine*, arXiv:cs.DB/0612123 [cs. DB], Cornell University Library, <http://www.arxiv.org/abs/cs.DB/0612123> (2006).
22. R. R. Anderson and J. A. Parrish, "The optics of human skin," *J. Invest. Dermatol.* **77**(1), 13–19 (1981).
23. S. Prael, "Optical Absorption of Hemoglobin," Oregon Medical Laser Center, <http://omlc.ogi.edu/spectra/hemoglobin/index.html> (15 December 1999).
24. W. Schwerd, *Der rote Blutfarbstoff und seine wichtigsten Derivate*, Schmidt-Römhild, Lübeck (1962).
25. G. Mie, "Beiträge zur Optik trüber Medien, speziell kolloidaler Metallösungen," *Ann. Phys.* **330**(3), 377–445 (1908).
26. H. C. van de Hulst, *Light Scattering by small Particles*, John Wiley & Sons, New York (1957).
27. F. P. Bolin et al., "Refractive index of some mammalian tissues using a fibre optic cladding method," *Appl. Opt.* **28**(12), 2297–2303 (1989).
28. K. Nassau, *The Physics and Chemistry of Colour*, 2nd ed., Wiley Series in Pure and Applied Optics, John Wiley & Sons, New York (2001).